We are IntechOpen, the world's leading publisher of Open Access books Built by scientists, for scientists

4,800
Open access books available

122,000
International authors and editors

135M
Downloads

Our authors are among the

154
Countries delivered to

TOP 1%
most cited scientists

12.2%
Contributors from top 500 universities

WEB OF SCIENCE™

Selection of our books indexed in the Book Citation Index in Web of Science™ Core Collection (BKCI)

Interested in publishing with us?
Contact book.department@intechopen.com

Numbers displayed above are based on latest data collected.
For more information visit www.intechopen.com

7

A Decentralized and Spatial Approach to the Robust Vibration Control of Structures

Alysson F. Mazoni, Alberto L. Serpa and Eurípedes G. de O. Nóbrega
University of Campinas - UNICAMP
Brazil

1. Introduction

Designing active controllers for minimizing mechanical vibration of structures is a challenging task which presents several levels of difficulties. Due to the continuous nature of the structures, they have an infinite number of degrees of freedom which leads to infinite vibration modes. This requires a model reduction and modal truncation considering the controller objectives, in order to achieve a viable numerical model which may allow the designed controller to perform satisfactorily within the frequency range of interest (Zhou & Doyle, 1997). But for real structures, even for truncated models, it may be expected a significant number of vibration modes to consider, conducting to mathematical and computational issues, besides the natural consequences of the reduction of the model order leading to unexpected behavior due to the controller feedback.

Considering the now vast literature in the vibration control area, there is no consensus regarding the most suitable control design method. Several techniques seem to give similar results, as shown in the works of Baz & Chen (2000); Bhattacharya et al. (2002); Hurlebaus et al. (2008). Linear matrix inequalities methods, due to powerful yet simple formulation and computational solution to implement the theory of robust control, present nowadays a slight predominance (Boyd et al., 1994; Zhou & Doyle, 1997). Several recent works that use this approach may be cited such as Barrault et al. (2007; 2008); Cheung & Wong (2009); Halim et al. (2008).

The $\mathcal{H}_\infty$ control technique emerged in the last decades as a robust control technique in the context of multiple-inputs and multiple-outputs (MIMO) feedback problems. The usual formulation involves the minimization of the $\mathcal{H}_\infty$ norm from the disturbances inputs to the performance outputs, corresponding to the minimization of the worst possible response. Vibration control of structures is a well reported application using this approach (Gawronski, 2004). Usually, performance outputs are selected based on the interest points distributed over the structure, and taken for the formulation of the objective function in the minimization problem.

However, the control problem, stated as the transfer matrix between the vibration actuator and sensor positions, has a known drawback. Because it does not clearly impose the desired behavior on the whole structure, it is not possible to guarantee the vibration level minimization beyond the sensor isolated position points. This approach may present acceptable reduction levels for simple structures, but more comprehensive methods are needed to achieve good results with real engineering structures, guaranteeing a vibration reduction through regions of the structure instead of isolated points.

The overall vibration energy distribution is then necessary to be considered, which renders the control problem always a non-collocated one. Additionally, real structures require in general a significant number of transducers, increasing the complexity of the system due to the number of transfer function combinations of inputs and outputs.

The spatial $\mathcal{H}_\infty$ control looks for an equivalent worst case output performance norm, in order to have a weighted performance over an specific region of the structure, instead of points. Addressing regions of interest instead of points, this methodology is attractive to the vibration control area. Particularly, for the common case of using a finite element model for the formulation of the spatial $\mathcal{H}_\infty$ control, it results in a simple formulation.

Some works have discussed the spatial $\mathcal{H}_\infty$ control, specially in the case of plate vibration (Halim, 2002; 2007; Halim et al., 2008). In these works, the spatial $\mathcal{H}_\infty$ design is solved trough a convenient algebraic manipulation which converts the spatial norm formulation to an equivalent ordinary $\mathcal{H}_\infty$ control problem.

Decentralized control is another promising approach recently studied for the vibration problem. Its basic architectural idea is to adopt several distributed controllers with lesser authority, instead of a big controller for the whole structure. Each controller accesses a subset of inputs and outputs, being responsible for a region of the structure. Decentralized control has been used for sound irradiation control of plates in Bianchi et al. (2004), with semi-active control in Casadei et al. (2010), using an optimal controller with static feedback in Jiang & Li (2010) and with decentralized velocity feedback in Zilletti et al. (2010). It is obviously useful for big structures in particular, where its constructive robustness represent an immediate advantage, since it may be implemented using independent microcontrollers and the system can easily accommodate actuator or sensor failures. Another advantage is the numerical simplicity of the controller algorithms, since each one deals with a smaller number of inputs and outputs. One problem is to decouple the controllers in order to avoid mutual undesired interference.

The purpose of this work is to compare an application of the spatial norm and the decentralized approaches to the vibration control of a plate including the $\mathcal{H}_\infty$ control technique, and adopting a linear matrix inequalities formulation.

The finite element method is used here to determine the vibration model of a plate. The plate is divided in Mindlin finite elements generating a discretized finite dimensional model that captures the vibration modes (Ferreira, 2008). The finite element method is suitable to determine the mass and stiffness matrices using interpolation functions of each finite element of the mesh, and the assemblage of these results for all the elements leads to a representation of the structure. This model is then used to generate the state-space model used to design the active controller.

This chapter is divided according to the following main topics: Structural modeling, where the main aspects of the dynamic equations, modal analysis fundamentals to describe the model, and model reduction are described; $\mathcal{H}_\infty$ control, where the optimization problem to minimize the $\mathcal{H}_\infty$ norm and aspects of multi-variable control are discussed; Spatial $\mathcal{H}_\infty$ control technique, where a more global and spatial vibration performance along the structure is considered as vibration reduction objective; Decentralized control, where controllers are designed in an independent form in order to reduce the design effort and also to increase the reliability in case of failures, is presented. Finally, the concluding remarks are presented.

The notation used in this work is: matrices are denoted by uppercase bold ($\mathbf{M}$, $\mathbf{K}$, $\mathbf{A}$ etc); vectors are denoted by lowercase bold ($\mathbf{x}$, $\mathbf{z}$, $\mathbf{y}$ etc); transposition of a matrix is denotes by the apostrophe (transpose of $\mathbf{C}$ is denoted by $\mathbf{C}'$ etc); time is denoted by variable t; frequency is denoted by ω.

2. Mechanical structures modeling

2.1 Dynamic equation

The movement equation of a generic structure can be written as

$$\mathbf{M}\ddot{\mathbf{q}}(t) + \mathbf{D}\dot{\mathbf{q}}(t) + \mathbf{K}\mathbf{q}(t) = \mathbf{B}_0\mathbf{f}(t), \tag{1}$$

where $\mathbf{q}(t)$ denotes the displacements, $\mathbf{M}$ is the mass matrix, $\mathbf{D}$ is the damping matrix, $\mathbf{K}$ is the stiffness matrix, $\mathbf{f}(t)$ is the vector of all external forces and $\mathbf{B}_0$ is a localization matrix for the external forces.

The main features of the dynamic response of a vibrating structure (Gawronski, 2004) are: 1) presence of resonance (amplification of response in specific frequencies); 2) the vibration models are decoupled (they can be excited independently); 3) the total response can be obtained by the summation of each mode contribution; 4) the impulse response consists of harmonic components, which are related to complex poles with small real parts; and 5) the system is controllable and observable.

2.2 Modal model

The structural model described in Eq. (1) can be represented also in modal coordinates (Ewins, 2000; Gawronski, 2004). The advantages of this kind of description are that the modal properties become evident such as the natural frequencies and damping factors for each structural mode.

The solution for the undamped free vibration is given by $\mathbf{q}(t) = \bar{\mathbf{q}}e^{j\omega t}$. Substituting this solution in the undamped free vibration movement equation it is obtained the eigen-problem given by

$$\mathbf{K}\bar{\mathbf{q}} = \omega^2\mathbf{M}\bar{\mathbf{q}}. \tag{2}$$

A structural system with n degrees of freedom presents n natural frequencies and n vibration modes. These natural frequencies and modes are determined through the solution of the eigen-problem related to the characteristic equation given by

$$det(\mathbf{K} - \omega^2\mathbf{M}) = 0 \tag{3}$$

The natural frequencies ω_i can be stored in a diagonal matrix $\mathbf{\Omega}$ given by

$$\mathbf{\Omega} = diag[\omega_1 \;\; \omega_2 \;\; \dots \;\; \omega_n], \tag{4}$$

and the vibration modes $\boldsymbol{\phi}_i$ can be stored in the matrix $\mathbf{\Phi}$ according to

$$\mathbf{\Phi} = [\boldsymbol{\phi}_1 \;\; \boldsymbol{\phi}_2 \;\; \dots \;\; \boldsymbol{\phi}_n]. \tag{5}$$

The model represented by the matrices $\mathbf{K}$ and $\mathbf{M}$ is the spatial model. The model denoted by the matrices $\mathbf{\Omega}$ and $\mathbf{\Phi}$ is the modal model.

A very important property is the orthogonality that allows the diagonalization of mass and stiffness matrices, i.e.,

$$\mathbf{\Phi}'\mathbf{M}\mathbf{\Phi} = diag[m_1 \;\; m_2 \;\; \dots \;\; m_n] = diag[m_i], \tag{6}$$

$$\mathbf{\Phi}'\mathbf{M}\mathbf{\Phi} = diag[k_1 \;\; k_2 \;\; \dots \;\; k_n] = diag[k_i]. \tag{7}$$

A specific situation which is mathematically convenient is the proportional damping where $\mathbf{D} = \alpha\mathbf{M} + \beta\mathbf{K}$. In this case it can be verified directly that the damping matrix is also

diagonalized since $\mathbf{M}$ and $\mathbf{K}$ can be diagonalized, i.e.,

$$\mathbf{\Phi}'\mathbf{D}\mathbf{\Phi} = \alpha\mathbf{\Phi}'\mathbf{M}\mathbf{\Phi} + \beta\mathbf{\Phi}'\mathbf{K}\mathbf{\Phi} = diag[d_1 \;\; d_2 \;\; \ldots \;\; d_n] = diag[d_i] \tag{8}$$

Considering a coordinate transformation given by $\mathbf{p}(t) = \mathbf{\Phi}\mathbf{q}(t)$, and pre-multiplying the Eq. (1) by $\mathbf{\Phi}$, it is possible to obtain for proportional damping

$$\mathbf{\Phi}'\mathbf{M}\mathbf{\Phi}\ddot{\mathbf{p}}(t) + \mathbf{\Phi}'\mathbf{D}\mathbf{\Phi}\dot{\mathbf{p}}(t) + \mathbf{\Phi}'\mathbf{K}\mathbf{\Phi}\mathbf{p}(t) = \mathbf{\Phi}'\mathbf{B}_0\mathbf{f}(t), \tag{9}$$

which can be rewriten as

$$diag[m_i]\ddot{\mathbf{p}}(t) + diag[d_i]\dot{\mathbf{p}}(t) + diag[k_i]\mathbf{p}(t) = \mathbf{\Phi}'\mathbf{B}_0\mathbf{f}(t) \tag{10}$$

One can verify that Eq. (10) corresponds to a set of uncoupled second order differential equations similar to the movement equation of the one degree of freedom system. Each decoupled equation corresponds to a specific vibration mode of the system and can be written as

$$m_i\ddot{p}_i(t) + d_i\dot{p}_i(t) + k_i p_i(t) = \bar{f}_i(t), \tag{11}$$

or in a standard form of second order system as

$$\ddot{p}_i(t) + 2\xi\omega_i\dot{p}_i(t) + \omega_i^2 p_i(t) = \gamma\omega_i^2\bar{f}_i(t). \tag{12}$$

It is possible to write for the i-mode the corresponding conjugate pair of poles

$$-\xi_i\omega_i \pm j\omega_i\sqrt{1-\xi_i^2} \tag{13}$$

where ω_i is the natural frequency and ξ_i is the non-dimensional damping factor, both related to the i vibration mode.
The modal model is a convenient way to include damping in models obtained by the finite element method, for example. The damping factor of each mode can be included independently. The proportional damping is not a mandatory hypothesis in this work since the control techniques can be applied to non-proportional damping also.

2.3 State-space model

The Eq. (1) can be rewriten as

$$\ddot{\mathbf{q}}(t) + \mathbf{M}^{-1}\mathbf{D}\dot{\mathbf{q}}(t) + \mathbf{M}^{-1}\mathbf{K}\mathbf{q}(t) = \mathbf{M}^{-1}\mathbf{B}_0\mathbf{f}(t). \tag{14}$$

Two kinds of external forces may be present in the active vibration control problem: the disturbance forces, denoted by $\mathbf{w}(t)$, and the control forces, denoted by $\mathbf{u}(t)$. Two kinds of outputs of the system can be defined: the measured outputs, denoted here by $\mathbf{y}(t)$, and the performance outputs, denoted by $\mathbf{z}(t)$.
Defining the state-space vector as $\mathbf{x}(t) = [\mathbf{q}(t) \;\; \dot{\mathbf{q}}(t)]'$, which corresponds to the displacements and velocities in this case, it is possible to write the state-space model in the form

$$\dot{\mathbf{x}}(t) = \mathbf{A}\mathbf{x}(t) + \mathbf{B}_1\mathbf{w}(t) + \mathbf{B}_2\mathbf{u}(t), \tag{15}$$

$$\mathbf{z}(t) = \mathbf{C}_1\mathbf{x}(t) + \mathbf{D}_{11}\mathbf{w}(t) + \mathbf{D}_{12}\mathbf{u}(t), \tag{16}$$

$$\mathbf{y}(t) = \mathbf{C}_2\mathbf{x}(t) + \mathbf{D}_{21}\mathbf{w}(t) + \mathbf{D}_{22}\mathbf{u}(t), \tag{17}$$

where the state-space matrix $\mathbf{A}$ is given by

$$\mathbf{A} = \begin{bmatrix} \mathbf{0} & \mathbf{I} \\ -\mathbf{M}^{-1}\mathbf{K} & -\mathbf{M}^{-1}\mathbf{K} \end{bmatrix}. \tag{18}$$

The matrices $\mathbf{B}_1$ and $\mathbf{B}_2$ are constructed with the structure $[\mathbf{0} \;\; \mathbf{M}^{-1}\mathbf{B}_0]'$ where the appropriate position matrix $\mathbf{B}_0$ is used for $\mathbf{w}(t)$ and for $\mathbf{u}(t)$. It is convenient to mention that the number of columns of $\mathbf{B}_1$ is the number of disturbances and the number of columns of $\mathbf{B}_2$ is the number of control forces.
The matrices $\mathbf{C}_1$, $\mathbf{D}_{11}$ and $\mathbf{D}_{12}$ are constructed to define the performance output in terms of the displacements, velocities and accelerations, or linear combinations of these values. The number of lines of $\mathbf{C}_1$ is the number of performances outputs to be monitored.
The matrices $\mathbf{C}_2$, $\mathbf{D}_{21}$ and $\mathbf{D}_{22}$ are constructed to specify the measured output also in terms of the displacements, velocities and accelerations. The number of lines of $\mathbf{C}_2$ is the number of measures.
This dynamic system can be represented in a compact form according to

$$\begin{bmatrix} \dot{\mathbf{x}}(t) \\ \mathbf{z}(t) \\ \mathbf{y}(t) \end{bmatrix} = \begin{bmatrix} \mathbf{A} & \mathbf{B}_1 & \mathbf{B}_2 \\ \mathbf{C}_1 & \mathbf{D}_{11} & \mathbf{D}_{12} \\ \mathbf{C}_2 & \mathbf{D}_{21} & \mathbf{D}_{22} \end{bmatrix} \begin{bmatrix} \mathbf{x}(t) \\ \mathbf{w}(t) \\ \mathbf{u}(t) \end{bmatrix}. \tag{19}$$

The transfer matrix of the system in Laplace domain variable s, relating each input to each output, can be writen as

$$\mathbf{P}(s) = \mathbf{C}(s\mathbf{I} - \mathbf{A})^{-1}\mathbf{B} + \mathbf{D}, \tag{20}$$

where

$$\mathbf{B} = [\mathbf{B}_1 \;\; \mathbf{B}_2], \quad \mathbf{C} = \begin{bmatrix} \mathbf{C}_1 \\ \mathbf{C}_2 \end{bmatrix}, \quad \mathbf{D} = \begin{bmatrix} \mathbf{D}_{11} & \mathbf{D}_{12} \\ \mathbf{D}_{21} & \mathbf{D}_{22} \end{bmatrix}. \tag{21}$$

2.4 State-space model in modal form

Considering that in modal coordinates the differential equations are decoupled for each mode, it is possible to reorganize the state-space in a modal form. Based on the standard form given by the Eq. (12), a state-space model for each mode can be generated.
One usual form of modal model (Gawronski, 2004) considers the states defined as

$$\mathbf{x}_i = \begin{bmatrix} \omega_i p_i \\ \xi_i \omega_i p_i + \dot{p}_i \end{bmatrix}. \tag{22}$$

For this case, the state-space matrix for the i-mode is given by

$$\mathbf{A}_i = \begin{bmatrix} -\xi_i\omega_i & \omega_i \\ -\omega_i & -\xi_i\omega_i \end{bmatrix}. \tag{23}$$

The state-space matrix will be a block diagonal matrix with the contribution of each mode in the form

$$\mathbf{A} = diag(\mathbf{A}_i). \tag{24}$$

This formulation is used in this work through the function `canon` with the option `modal` in the MATLAB® software.

2.5 Model reduction

A real structure is a continuous system with infinite degrees of freedom. It is necessary to have a finite dimensional representation for the system. This representation can be obtained by techniques such as finite elements or direct experimental identification. These two approaches lead to models that are finite dimensional but that can present a number of degrees of freedom yet considered excessive large. In this case, in order to have a feasible numerical treatment and feasible controller design, it is necessary to have a reduced order model.

The model reduction can be performed according to some techniques (Qu, 2004). The most usual and simple technique is the model truncation, where a number of modes is kept under a critical frequency value of interest. Upper frequency modes are simply discarded. This technique is adequate for the objectives of this work, and it is adopted here. Obviously the lost information can affect the dynamic representation of the structure and bring undesirable effects, such as spillover, implying the use of additional performance filtering to the model. In most situations, the interest in the dynamic response of the structure is limited to a specific range of frequencies, and the model reduction can be performed considering this information. In the present case, the model reduction is conducted using the function `modreal` of the software MATLAB. This function performs the model reduction selecting the frequency ordered blocks of the modal model corresponding to the indicated frequency range, i.e., the selection is based on the blocks of the Eq. (24).

3. Structural and control models - plate vibration

It is considered in this work a finite element model of a plate. The MATLAB codes given in Ferreira (2008) were employed to obtain the mass and stiffness matrices considering the Mindlin plate formulation. The plate finite element has four nodes and three degrees of freedom in each node: rotations in axes x and y and displacement in axis z. The plate in this work was considered with all boundaries free. The finite element mesh is shown in Figure 1, and Table 1 shows the physical parameters used in the finite element model of the plate.

This finite element model presents 90 nodes with 3 degrees of freedom per node. This leads to a model of 270 degrees of freedom and 540 states. This model was reduced to a model with 24 states for control design purposes.

This model is used in this work to evaluate the spatial and decentralized $\mathcal{H}_\infty$ control techniques. There are, in this plate model, three convenient orientations for the transducers: horizontal, vertical and with an orientation of 45 degrees (representing identical actuation in the degrees of freedom in x and y directions of the same node). The placement of these sensors and actuators are indicated in Figure 1.

Height	1 m
Width	1 m
Thickness	2 mm
Density	2710 kg/m^3
Poisson Modulus	0.33
Young Modulus	70 GPa

Table 1. Physical properties of the plate

In order to have a more realistic dynamic system in the simulations, damping should be taken into account. In this case, it was included a modal damping of 3×10^{-6} to all vibration modes of the plate.

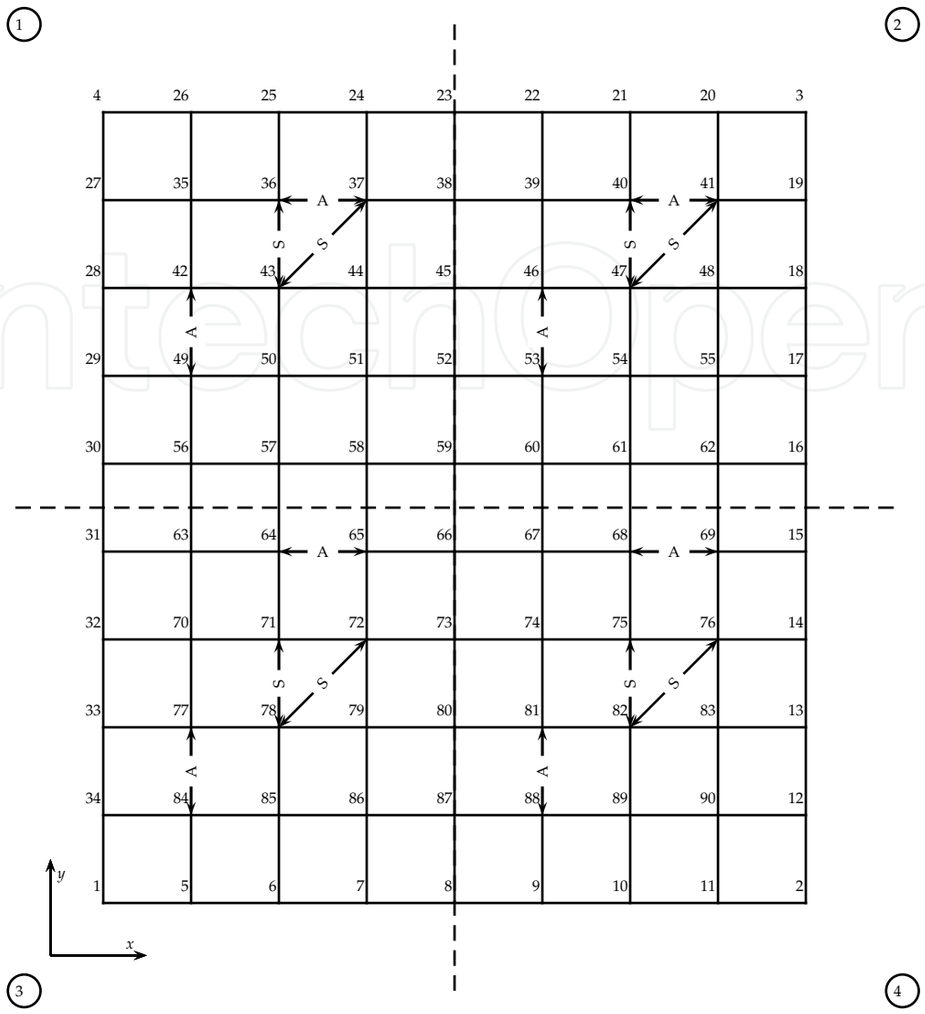

Fig. 1. Finite element mesh for the plate with four partitions - A denotes actuators and S denotes sensors

It is considered that the actuators and sensors are piezoelectric (PZT). The actuator receives a voltage and apply a pair of opposite moments in nearby nodes. The sensor generates a voltage proportional to its deformation, i.e., proportional to the difference between angles in nearby nodes. Figure 2 shows schematically the actuator and sensor representation used in this work.

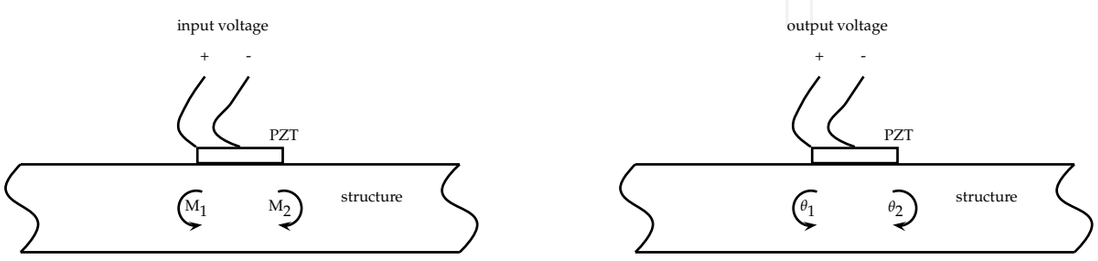

Fig. 2. PZT actuator and sensor relations to the respective degrees-of-freedom

	Actuators			Sensors		
	Number	DOF	Nodes	Number	DOF	Nodes
Disturbance	1 (w)	$\odot$	86			
Partition 1	2 (u_1)	$\leftrightarrow$	36 - 37	1 (z_1)	$\swarrow\!\!\nearrow$	43 - 37
	3 (u_2)	$\updownarrow$	49 - 42	2 (y_1)	$\updownarrow$	43 - 36
Partition 2	4 (u_3)	$\leftrightarrow$	40 - 41	3 (z_2)	$\swarrow\!\!\nearrow$	47 - 41
	5 (u_4)	$\updownarrow$	53 - 46	4 (y_2)	$\updownarrow$	47 - 40
Partition 3	6 (u_5)	$\leftrightarrow$	64 - 65	5 (z_3)	$\swarrow\!\!\nearrow$	78 - 72
	7 (u_6)	$\updownarrow$	84 - 77	6 (y_3)	$\updownarrow$	78 - 71
Partition 4	8 (u_7)	$\leftrightarrow$	68 - 69	7 (z_4)	$\swarrow\!\!\nearrow$	82 - 76
	9 (u_8)	$\updownarrow$	88 - 81	8 (y_4)	$\updownarrow$	82 - 75

Table 2. Definition and placement of actuators and sensors for the mesh in the Figure 1.

Table 2 shows actuators, sensors and nodes location for the mesh of Figure 1. The arrows indicate the respective degrees of freedom. The partition reveals which actuators and sensors are used in each local model for the case of the decentralized control. The disturbance is considered a force in the z direction applied in the node 86. Actuators numbered from 2 to 9 are chosen as control inputs. Sensors 2, 4, 6 and 8 are measuring outputs. The performance parameters are the sensors numbered as 1, 3, 5 and 7. The uncontrolled system was normalized to have an $\mathcal{H}_\infty$ norm equal to 1 (normalized plant).

4. $\mathcal{H}_\infty$ control formulation

The $\mathcal{H}_\infty$ control design method consists of designing a controller transfer function $\mathbf{K}(s)$ in a closed loop with a plant $\mathbf{P}(s)$ in order to minimize the $\mathcal{H}_\infty$ norm of the closed loop transfer function $\mathbf{T}(s)$ from the disturbance $\mathbf{w}$ to the performance $\mathbf{z}$ in the frequency domain ω. The loop is usually represented as in Figure 3.

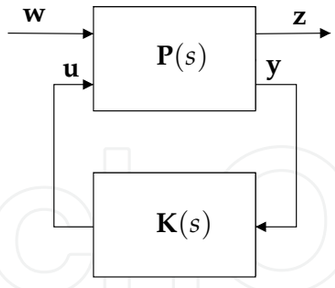

Fig. 3. $\mathcal{H}_\infty$ closed loop diagram

The $\mathcal{H}_\infty$ norm of a system, from the disturbance input $\mathbf{w}(t)$ to the performance output $\mathbf{z}(t)$ (Skelton et al., 1998), can be defined as

$$J_\infty = \|\mathbf{T}(s)\|_\infty = \frac{\int_0^\infty \mathbf{z}'(t)\mathbf{z}(t)\,dt}{\int_0^\infty \mathbf{w}'(t)\mathbf{w}(t)dt}. \tag{25}$$

The $\mathcal{H}_\infty$ norm can be calculated as

$$\|\mathbf{T}(s)\|_\infty = \sup_\omega \bar{\sigma}(\mathbf{T}(j\omega)),$$

where $\bar{\sigma}$ is the maximum singular value of the transfer function $\mathbf{T}(s)$ (Zhou & Doyle, 1997). This is a measure in the frequency domain of the worst response of $\mathbf{T}(s)$. If the worst response, in the sense of the higher amplitude, is achieved to an acceptable level, the performance is evidently guaranteed for all cases.

Weighting functions are used in this work to compel the performance output and control signals to follow the specified frequency distributions. In general, low-pass weighting functions $W_z(s)$ are used to balance the performance output levels and high-pass functions $W_u(s)$ are applied to the control forces. Commonly used filter functions (Zhou & Doyle, 1997) are:

$$W_p(s) = \left(\frac{s\sqrt[k]{M} + \omega_c}{s + \omega_c \sqrt[k]{\epsilon}} \right)^k, \qquad W_u(s) = \left(\frac{s + \omega_c \sqrt[k]{M}}{s\sqrt[k]{\epsilon} + \omega_c} \right)^k,$$

where ω_c is the cut frequency, k is the filter order, M is the gain at pass band and ϵ is the gain at rejection band.

Specifying the correct weighting functions for each problem is very important in the controller design process. They define the frequency regions where the disturbance signals response should be minimized and where the control signals should be effective, avoiding the excitation of neglected vibration modes in the model, which is fundamental to avoid the spillover effect (Balas, 1978).

An $\mathcal{H}_\infty$ controller design problem can be written as an optimization problem. The controller $\mathbf{K}(s)$ can be obtained by the minimization of the $\mathcal{H}_\infty$ norm of the closed-loop $\mathbf{T}(s)$, i.e.,

$$\begin{array}{rl} \min_{\mathbf{K}(s)} & \|\mathbf{T}(s)\|_\infty \\ \text{subjected to} & \mathbf{K}(s) \text{ stable} \\ & \mathbf{T}(s) \text{ stable.} \end{array}$$

This optimization problem can be considered a global design, since it involves all the inputs and outputs of the plant. Provided an acceptable level of vibration, a sub-optimal solution of this problem may be obtained solving the associated Riccati equations or by the solution of a linear matrix inequality problem (Boyd et al., 1994; Zhou & Doyle, 1997). The solution of this problem can be obtained using the MATLAB Robust Control Toolbox with the `hinfsyn` function for example.

5. Spatial $\mathcal{H}_\infty$ control

5.1 Spatial $\mathcal{H}_\infty$ norm

The $\mathcal{H}_\infty$ norm may be generalized considering a spatial distribution for the performance parameters. This can lead to a weighted response over the specified spatial region.

The spatial $\mathcal{H}_\infty$ norm (Skelton et al., 1998) for a dynamic system considering the disturbance input $\mathbf{w}(t)$ to the spatial performance output $\mathbf{z}(r,t)$ can be defined as

$$J_\infty = \frac{\int_0^\infty \int_{\mathcal{R}} \mathbf{z}'(t,r)\mathbf{Q}(r)\mathbf{z}(t,r)\, dr dt}{\int_0^\infty \mathbf{w}'(t)\mathbf{w}(t)\, dt}, \tag{26}$$

where $\mathcal{R}$ denotes the spatial region and $\mathbf{Q}(r)$ is a spatial weighting function.

5.2 Spatial and non-spatial $\mathcal{H}_\infty$-control parallel

The spatial $\mathcal{H}_\infty$ norm allows to generalize the $\mathcal{H}_\infty$ control design problem. Consider a system in which the performance output $\mathbf{z}(r,t)$ depends both on space (r) and time (t), whilst the

measured output $\mathbf{y}(t)$ depends only on time. The state space model may be described as:

$$\begin{aligned} \dot{\mathbf{x}}(t) &= \mathbf{A}\mathbf{x}(t) + \mathbf{B}_1\mathbf{w}(t) + \mathbf{B}_2\mathbf{u}(t) \\ \mathbf{z}(t,r) &= \mathbf{C}_1(r)\mathbf{x}(t) + \mathbf{D}_{11}(r)\mathbf{w}(t) + \mathbf{D}_{12}(r)\mathbf{u}(t) \\ \mathbf{y}(t) &= \mathbf{C}_2 x(t) + \mathbf{D}_{21}\mathbf{w}(t) + \mathbf{D}_{22}\mathbf{u}(t). \end{aligned} \tag{27}$$

It is possible to notice that r stands for a vector position and can represent two or three-dimensional problems. The definition of the spatial norm is a multiple integral depending on the problem dimensionality according to the Eq. (26).
The purpose of control design is to obtain a dynamic controller given by

$$\begin{aligned} \dot{\mathbf{x}}_k(t) &= \mathbf{A}_k\mathbf{x}_k(t) + \mathbf{B}_k y(t) \\ \mathbf{u}(t) &= \mathbf{C}_k\mathbf{x}_k(t) + \mathbf{D}_k\mathbf{y}(t), \end{aligned}$$

which reduces the particular norm of interest.
The spatial $\mathcal{H}_\infty$ problem is solved through the conversion to an equivalent punctual $\mathcal{H}_\infty$ with a modified performance output $\tilde{\mathbf{z}}(t)$, which is responsible for taking into account the desired vibration region. The ordinary $\mathcal{H}_\infty$ norm based on $\tilde{\mathbf{z}}(t)$ according to Equation (25) is

$$J_\infty = \frac{\int_0^\infty \tilde{\mathbf{z}}'(t)\tilde{\mathbf{z}}(t)\,dt}{\int_0^\infty \mathbf{w}'(t)\mathbf{w}(t)\,dt}. \tag{28}$$

Comparing equations (28) and (26) it is possible to establish the equivalence

$$\tilde{\mathbf{z}}'(t)\tilde{\mathbf{z}}(t) = \int_{\mathcal{R}} \mathbf{z}'(t,r)\mathbf{Q}(r)\mathbf{z}(r,t)\,dr. \tag{29}$$

This equivalence allows to convert the spatial $\mathcal{H}_\infty$ control design problem into the standard $\mathcal{H}_\infty$ problem with the modified performance output.
From Equation (27):

$$\mathbf{z}(t,r) = \begin{bmatrix} \mathbf{C}_1(r) & \mathbf{D}_{11}(r) & \mathbf{D}_{12}(r) \end{bmatrix} \begin{bmatrix} \mathbf{x} \\ \mathbf{w} \\ \mathbf{u} \end{bmatrix},$$

and the equivalent punctual output

$$\tilde{\mathbf{z}}(t) = \mathbf{\Gamma} \begin{bmatrix} \mathbf{x} \\ \mathbf{w} \\ \mathbf{u} \end{bmatrix}. \tag{30}$$

Using Equation (29), it is possible to write

$$\begin{bmatrix} \mathbf{x} \\ \mathbf{w} \\ \mathbf{u} \end{bmatrix}' \mathbf{\Gamma}'\mathbf{\Gamma} \begin{bmatrix} \mathbf{x} \\ \mathbf{w} \\ \mathbf{u} \end{bmatrix} =$$

$$= \int_{\mathcal{R}} \begin{bmatrix} \mathbf{x} \\ \mathbf{w} \\ \mathbf{u} \end{bmatrix}' \begin{bmatrix} \mathbf{C}_1'(r) \\ \mathbf{D}_{11}'(r) \\ \mathbf{D}_{12}'(r) \end{bmatrix} \mathbf{Q}(r) \begin{bmatrix} \mathbf{C}_1(r) & \mathbf{D}_{11}(r) & \mathbf{D}_{12}(r) \end{bmatrix} \begin{bmatrix} \mathbf{x} \\ \mathbf{w} \\ \mathbf{u} \end{bmatrix} dr,$$

$$\begin{bmatrix} \mathbf{x} \\ \mathbf{w} \\ \mathbf{u} \end{bmatrix}' \boldsymbol{\Gamma}'\boldsymbol{\Gamma} \begin{bmatrix} \mathbf{x} \\ \mathbf{w} \\ \mathbf{u} \end{bmatrix} =$$

$$= \begin{bmatrix} \mathbf{x} \\ \mathbf{w} \\ \mathbf{u} \end{bmatrix}' \int_{\mathcal{R}} \begin{bmatrix} \mathbf{C}_1'(r) \\ \mathbf{D}_{11}'(r) \\ \mathbf{D}_{12}'(r) \end{bmatrix} \mathbf{Q}(r) \left[\mathbf{C}_1(r) \;\; \mathbf{D}_{11}(r) \;\; \mathbf{D}_{12}(r)\right] dr \begin{bmatrix} \mathbf{x} \\ \mathbf{w} \\ \mathbf{u} \end{bmatrix}.$$

The equivalence results in the following equality

$$\boldsymbol{\Gamma}'\boldsymbol{\Gamma} =$$

$$= \int_{\mathcal{R}} \begin{bmatrix} \mathbf{C}_1'(r) \\ \mathbf{D}_{11}'(r) \\ \mathbf{D}_{12}'(r) \end{bmatrix} \mathbf{Q}(r) \left[\mathbf{C}_1(r) \;\; \mathbf{D}_{11}(r) \;\; \mathbf{D}_{12}(r)\right] dr. \tag{31}$$

By defining a spatial weighting function $\mathbf{Q}(r)$, the matrix $\boldsymbol{\Gamma}'\boldsymbol{\Gamma}$ can be found from Equation (31) and $\boldsymbol{\Gamma}$ may be determined. One should notice that $\boldsymbol{\Gamma}$ is the transformation that allows the punctual $\mathcal{H}_\infty$ problem to represent equivalently the spatial $\mathcal{H}_\infty$ problem.
Using Equation (30), the performance output $\tilde{\mathbf{z}}$ is defined as

$$\tilde{\mathbf{z}} = \boldsymbol{\Gamma} \begin{bmatrix} \mathbf{x} \\ \mathbf{w} \\ \mathbf{u} \end{bmatrix} = \left[\boldsymbol{\Pi} \;\; \boldsymbol{\Theta}_1 \;\; \boldsymbol{\Theta}_2\right] \begin{bmatrix} \mathbf{x} \\ \mathbf{w} \\ \mathbf{u} \end{bmatrix},$$

in which $\boldsymbol{\Pi}$, $\boldsymbol{\Theta}_1$ and $\boldsymbol{\Theta}_2$ are simultaneously defined as matrix partitions of $\boldsymbol{\Gamma}$ according to the signal dimensions.
So, the final plant model is written as

$$\begin{aligned} \dot{\mathbf{x}}(t) &= \mathbf{A}\mathbf{x}(t) + \mathbf{B}_1\mathbf{w}(t) + \mathbf{B}_2\mathbf{u}(t) \\ \tilde{\mathbf{z}}(t) &= \boldsymbol{\Pi}\mathbf{x}(t) + \boldsymbol{\Theta}_1\mathbf{w}(t) + \boldsymbol{\Theta}_2\mathbf{u}(t) \\ \mathbf{y}(t) &= \mathbf{C}_2\mathbf{x}(t) + \mathbf{D}_{21}\mathbf{w}(t) + \mathbf{D}_{22}\mathbf{u}(t). \end{aligned}$$

5.3 Calculation of $\boldsymbol{\Gamma}$

Equation (31) defines $\boldsymbol{\Gamma}'\boldsymbol{\Gamma}$ as an integral of a square matrix of order $n + n_w + n_u$, where n is the number of plant states, n_w is the number of disturbances and n_u is the number of control signals. $\boldsymbol{\Gamma}$ has dimensions $p \times (n + n_w + n_u)$, where the number of lines p represents the number of performance outputs, i.e., the number of lines of $\tilde{\mathbf{z}}$. The number of elements of $\boldsymbol{\Gamma}$ is $p \times (n + n_w + n_u)$ and the number of elements of $\boldsymbol{\Gamma}'\boldsymbol{\Gamma}$ is $(n + n_w + n_u) \times (n + n_w + n_u)$. Since, $\boldsymbol{\Gamma}'\boldsymbol{\Gamma}$ is symmetric, the number of unknowns elements are $(n + n_w + n_u)(n + n_w + n_u + 1)/2$. A convenient choice is $p = n + n_w + n_u$, which amounts to a square matrix for $\boldsymbol{\Gamma}$, and in this case a Cholesky factorization can be applied in $\boldsymbol{\Gamma}'\boldsymbol{\Gamma}$ to obtain $\boldsymbol{\Gamma}$. Another possibility to determine Γ involves a specific situation related to finite element models as described in the next section.

5.4 Γ for the case of constant spatial weighting

Taking the spatial weighting function constant inside every element allows some simplifying results. In this case the spatial performance output can be discretized for the degrees of freedom that are the model states and the spatial performance output can be interpolated from the degrees of freedom. The integral of Equation (31) that defines $\boldsymbol{\Gamma}'\boldsymbol{\Gamma}$ may be approximated

as

$$\mathbf{\Gamma}'\mathbf{\Gamma} \approx \sum_i f(r_i) \begin{bmatrix} \mathbf{C}_1'(r_i) \\ \mathbf{D}_{11}'(r_i) \\ \mathbf{D}_{12}'(r_i) \end{bmatrix} \mathbf{Q}(r_i) \left[\mathbf{C}_1(r_i) \;\; \mathbf{D}_{11}(r_i) \;\; \mathbf{D}_{12}(r_i)\right], \tag{32}$$

by supposing an integration method such as the gaussian quadrature (Bathe, 1995), where the values $f(r_i)$ represent the contribution to the specific degree of freedom. In this case, $f(r_i)$ can be considered the gauss weightings and r_i the respective integration points (in this case the degrees of freedom).
If the finite element mesh is homogeneous in terms of the element size, a simplification of a constant value of the integrand inside each element can be used leading to less calculations. The integral in Equation (31) becomes a summation according to

$$\mathbf{\Gamma}'\mathbf{\Gamma} = \sum_i \begin{bmatrix} \mathbf{C}_{1i}' \\ \mathbf{D}_{11i}' \\ \mathbf{D}_{12i}' \end{bmatrix} Q_i \left[\mathbf{C}_{1i} \;\; \mathbf{D}_{11i} \;\; \mathbf{D}_{12i}\right] A_i, \tag{33}$$

with A_i as an elementary length, area or volume, according to the dimension in the integral, and Q_i is the weighting function value related to point i in Equation (32). A simplification of notation, taking i to denote the corresponding r_i, was employed.
Defining $t_i = Q_i A_i$, it is possible to write Equation (33) as

$$\mathbf{\Gamma}'\mathbf{\Gamma} = \sum_i \left(\begin{bmatrix} \mathbf{C}_{1i}' \\ \mathbf{D}_{11i}' \\ \mathbf{D}_{12i}' \end{bmatrix} \sqrt{t_i} \right) \left(\sqrt{t_i} \left[\mathbf{C}_{1i} \;\; \mathbf{D}_{11i} \;\; \mathbf{D}_{12i}\right] \right).$$

This summation can be rewritten as

$$\mathbf{\Gamma}'\mathbf{\Gamma} = \left(\sum_i \sqrt{t_i} \begin{bmatrix} \mathbf{C}_{1i}' \\ \mathbf{D}_{11i}' \\ \mathbf{D}_{12i}' \end{bmatrix} \right) \left(\sum_i \sqrt{t_i} \left[\mathbf{C}_{1i} \;\; \mathbf{D}_{11i} \;\; \mathbf{D}_{12i}\right] \right) - \mathbf{X},$$

where

$$\mathbf{X} = \sum_i \sum_j^{i \neq j} t_i \begin{bmatrix} \mathbf{C}_{1i}' \\ \mathbf{D}_{11i}' \\ \mathbf{D}_{12i}' \end{bmatrix} \left[\mathbf{C}_{1j} \;\; \mathbf{D}_{11j} \;\; \mathbf{D}_{12j}\right].$$

Since finite element models are considered in this work, where the degrees of freedom are model states, the matrices $\left[\mathbf{C}_{1j} \;\; \mathbf{D}_{11j} \;\; \mathbf{D}_{12j}\right]$ are orthogonal. $\mathbf{C}_{1j}$ is a matrix of zeros with a one in the position j of the convenient degree of freedom. $\mathbf{D}_{11j}$ and $\mathbf{D}_{12j}$ are null since the displacement and velocities are the states. Acceleration outputs are not considered in this work. This yields $\mathbf{X} = \mathbf{0}$ and consequently

$$\mathbf{\Gamma}'\mathbf{\Gamma} = \left(\sum_i \sqrt{t_i} \begin{bmatrix} \mathbf{C}_{1i}' \\ \mathbf{D}_{11i}' \\ \mathbf{D}_{12i}' \end{bmatrix} \right) \left(\sum_i \sqrt{t_i} \left[\mathbf{C}_{1i} \;\; \mathbf{D}_{11i} \;\; \mathbf{D}_{12i}\right] \right)$$

where one can choose

$$\Gamma = \sum_i \sqrt{t_i} \left[\mathbf{C}_{1i} \;\; \mathbf{D}_{11i} \;\; \mathbf{D}_{12i}\right]. \tag{34}$$

In this way, a numerical definition of the output matrix $\mathbf{\Gamma}$ of the $\mathcal{H}_\infty$ spatial control is achieved for the particular case of finite element models, where the degrees of freedom are the states.

6. Decentralized $\mathcal{H}_\infty$ control

The decentralized control design problem can be obtained by imposing a block-diagonal structure to the controller. If the order of inputs and outputs in the transfer function respects physical proximity, a block diagonal structure for the controller can be obtained such as:

$$\mathbf{K}(s) = \begin{bmatrix} \mathbf{K}_1(s) & & & \\ & \mathbf{K}_2(s) & & \\ & & \ddots & \\ & & & \mathbf{K}_p(s) \end{bmatrix},$$

where $\mathbf{K}_i(s)$ are the local controllers.
It is difficult to formulate the decentralized control design with a problem structure that can be solved easily. When the optimization problem is formulated through linear matrix inequalities, the requirement to impose a particular structure in the decision variable $\mathbf{K}(s)$ represents a mathematical difficulty that can lead to a non-convex problem. This difficulty motivates the investigation of other approaches for the decentralized control.
One alternative is that the original plant can be divided in several local plants with their own inputs and outputs and with spatially close actuators and sensors. In this case, it is possible to design local controllers corresponding to each plant subdivision. The closed-loop can be generated by employing these controllers along with the original plant in all its input and output signals, i.e., it is possible to solve several optimization problems such as

$$\begin{array}{rl} \min_{\mathbf{K}_i(s)} & \|\mathbf{T}_i(s)\|_\infty \\ \text{subjected to} & \mathbf{K}_i(s) \text{ stable} \\ & \mathbf{T}_i(s) \text{ stable.} \end{array}$$

where the controllers $\mathbf{K}_i(s)$ are obtained. In this case, the closed-loop is a function of all controllers and of the global plant.
Through this approach no additional mathematical development is necessary, since the solution is taken as a combination of solutions of several simultaneous optimizations problems.

7. Simulated results

Using $\mathcal{H}_\infty$ control for both the centralized and decentralized designs the same configuration of actuators and sensors already described were adopted in order to permit to compare the results.
The control design is performed using the linear matrix inequalities formulation for the $\mathcal{H}_\infty$ controller design using the function `hinfsyn` of MATLAB 7.2 (default parameters).
The parameters of the weighting filters used in this work are shown in Table 3. The same filters were employed in all simulations of this work.
A simulation test is performed according to the presented configuration of inputs and outputs. A linear sine sweep of 10 s from 0 to 2 KHz is used as a disturbance signal in all cases.

	ω_c	k	M	ϵ
$W_z(s)$ - low-pass weight for performance	1500	1	0.1	0.001
$W_u(s)$ - high-pass weight for control force	2000	1	0.1	0.001

Table 3. Weighting filters parameters

7.1 Centralized control

The centralized control case is the ordinary punctual $\mathcal{H}_\infty$ applied to the finite element model of the plate described above. Control results for the centralized control are shown in time domain in Figure 4 and in frequency domain in Figure 5.

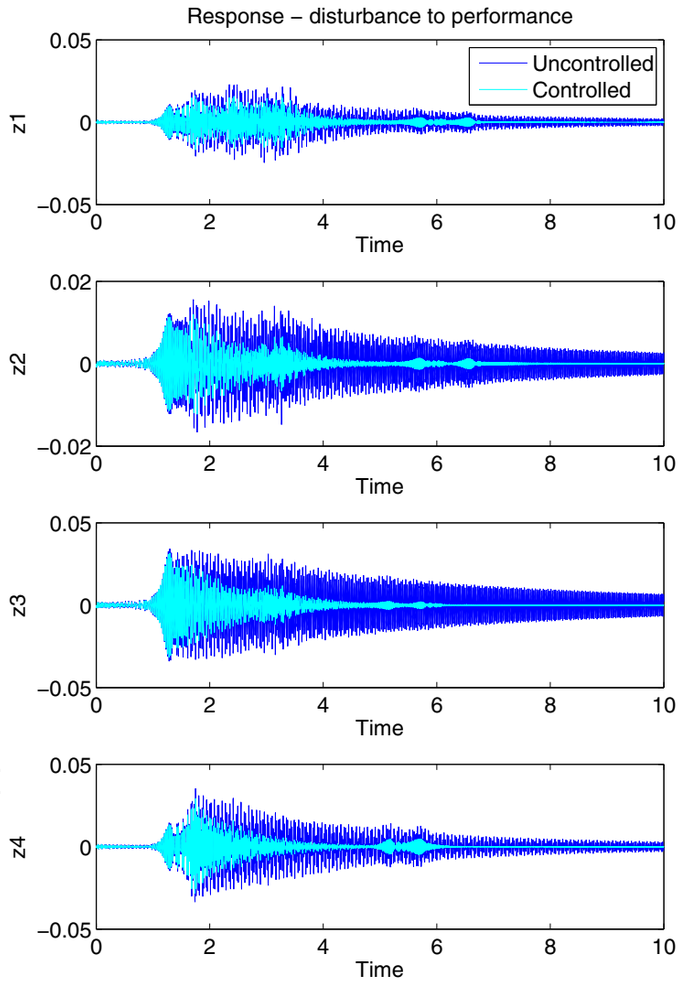

Fig. 4. Centralized control - control result from disturbance signal to spatial performance output

The time scale in Figure 4 is the duration of the sweep disturbance signal, and it may be interpreted as a frequency scale. It is possible to observe a good attenuation increasing as the

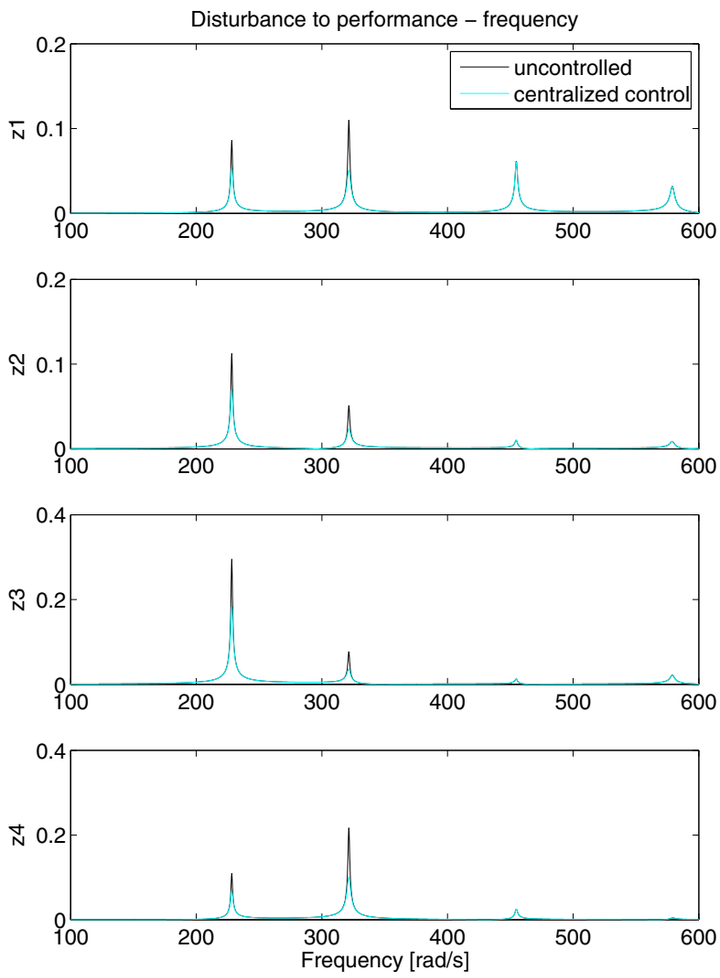

Fig. 5. Centralized control - control result from disturbance signal to spatial performance output in frequency domain

disturbance frequency increases. It is possible to notice also the presence of four predominant natural frequencies in the plate, but only in the attenuated response.
In the spectral response of Figure 5 it is possible to observe clearly the four natural frequencies, but only the first and the second peaks are attenuated, achieving a reduction of approximately 50% in the amplitude. The bigger reduction on the time response of Figure 4 for the highest frequencies is due to the low damping regularly found in these structures, and the respective transient response.

7.2 Decentralized control

Frequency and time domain results for the decentralized control in contrast with centralized control are shown in Figures 6 and 7.
In Figure 6 it is possible to see that the attenuation of the decentralized controller is practically the same, but just a bit less amplitude is present in the middle frequencies.

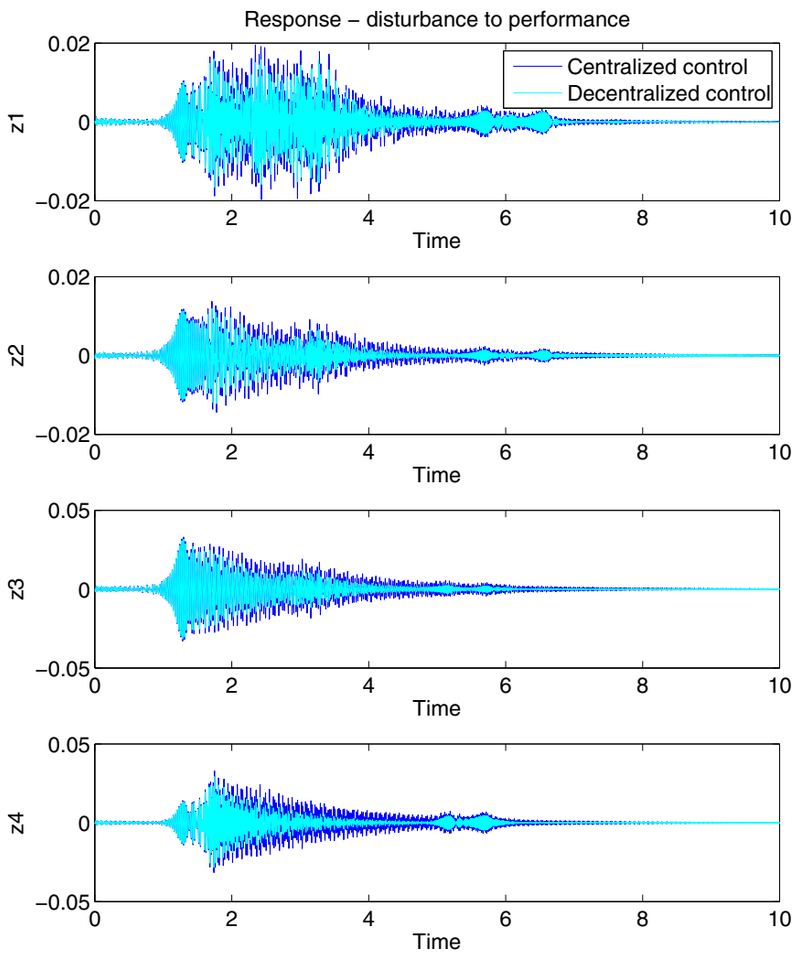

Fig. 6. Centralized and decentralized control - control result from disturbance signal to spatial performance output

In Figure 7 this slightly bigger attenuation is not present in any of the four peaks, with a complete superposition of the responses. Once again, the difference seen in Figure 6 is due to the low damping of the plate.

7.3 Spatial control

In the spatial control case the performance is the spatial output defined in the original design, which in this case is a constant and equal weighting of all the nodes except for the boundary of the plate.

The first four sensors are used as performance measurements with the same control loop design for the spatial performance defined for the whole plate, in order to compare it with $\mathcal{H}_\infty$ decentralized design. The control results obtained are shown in frequency and time response respectively in Figures 8 and 9.

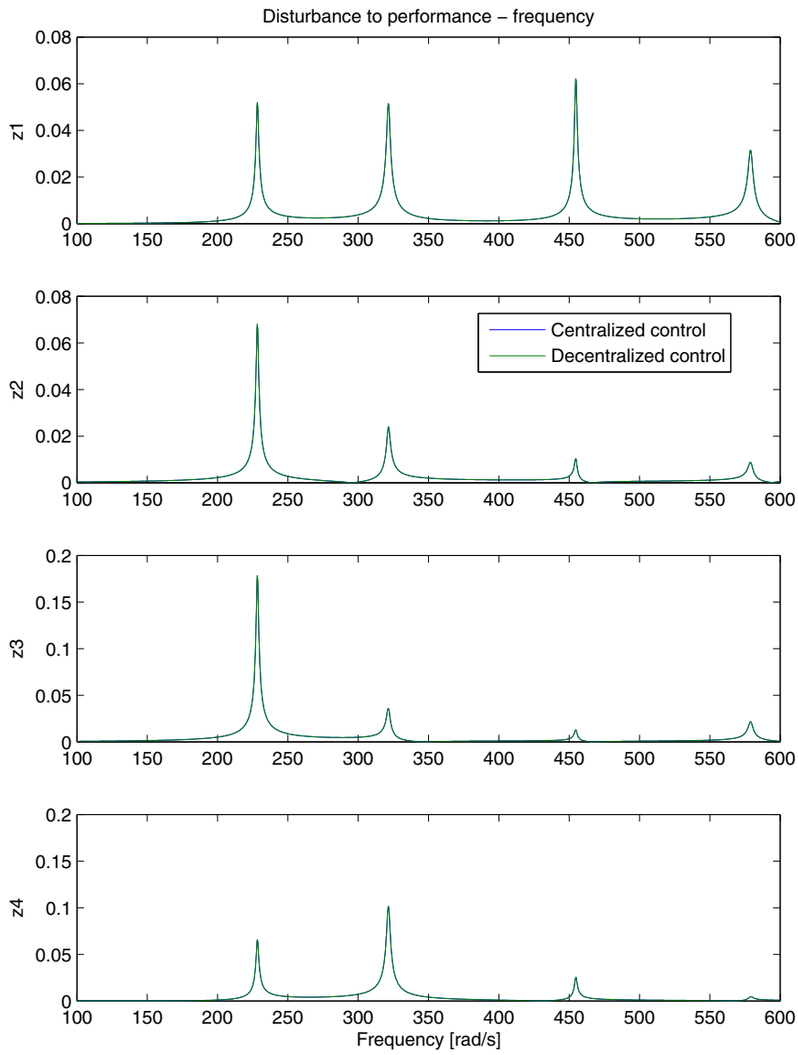

Fig. 7. Centralized and decentralized control - control result from disturbance signal to spatial performance output in frequency domain

In Figure 8 it is possible to notice that the spatial attenuation is bigger than in the decentralized controller results, in the low and middle frequency regions.
In Figure 9 the attenuation attained by the spatial controller is on the range around 10 and 20%, in comparison to the decentralized controller, which presented a similar result to the centralized controller on the order of 50%. This means that the spatial controller achieved indeed a good vibration attenuation result. But in the high frequency range, the two peaks once again were not attenuated.

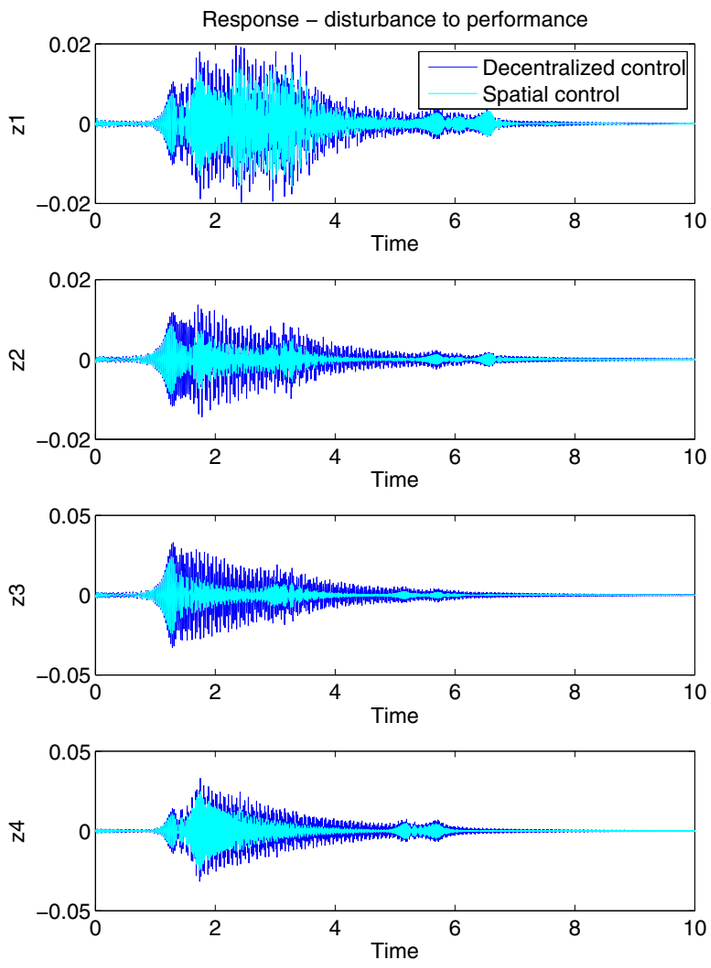

Fig. 8. Decentralized and spatial control - control results from disturbance signal to spatial performance outputs

7.4 Control signal comparison

The control signal levels for the spatial and decentralized controlled are presented in Figure 10 in the time domain. It is possible to have some insight into the behavior of the controllers results by analyzing these curves.

The closed loop frequency response, through the associated controllers efforts to attenuate the correspondent natural frequencies, is very clear on the curves of Figure 10. The spatial controller presented a bigger effort to attenuate the first and the second peaks, while the level of the decentralized controller does not reflect clearly the passage of the natural frequencies. That is the reason that made the spatial controller the better one. Other higher frequencies also presented controller effort, but the respective attenuation was not possible to be seen in the spectral responses in Figure 9. It would be interesting to further investigate if some other points of the region is presenting attenuation on these peaks.

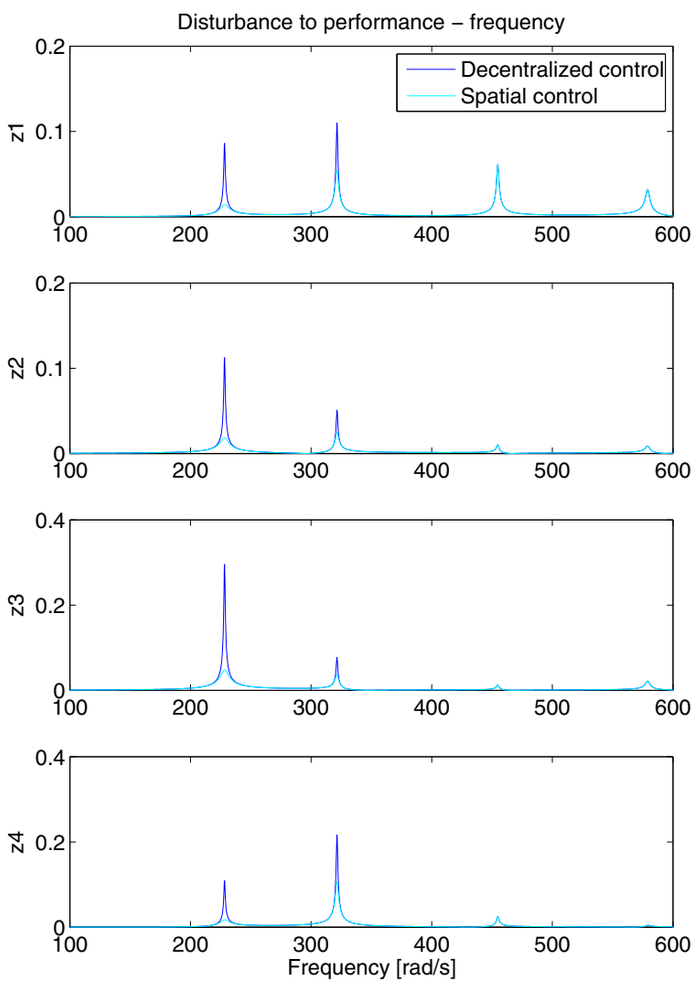

Fig. 9. Decentralized and spatial control - control results from disturbance signal to spatial performance outputs in frequency domain

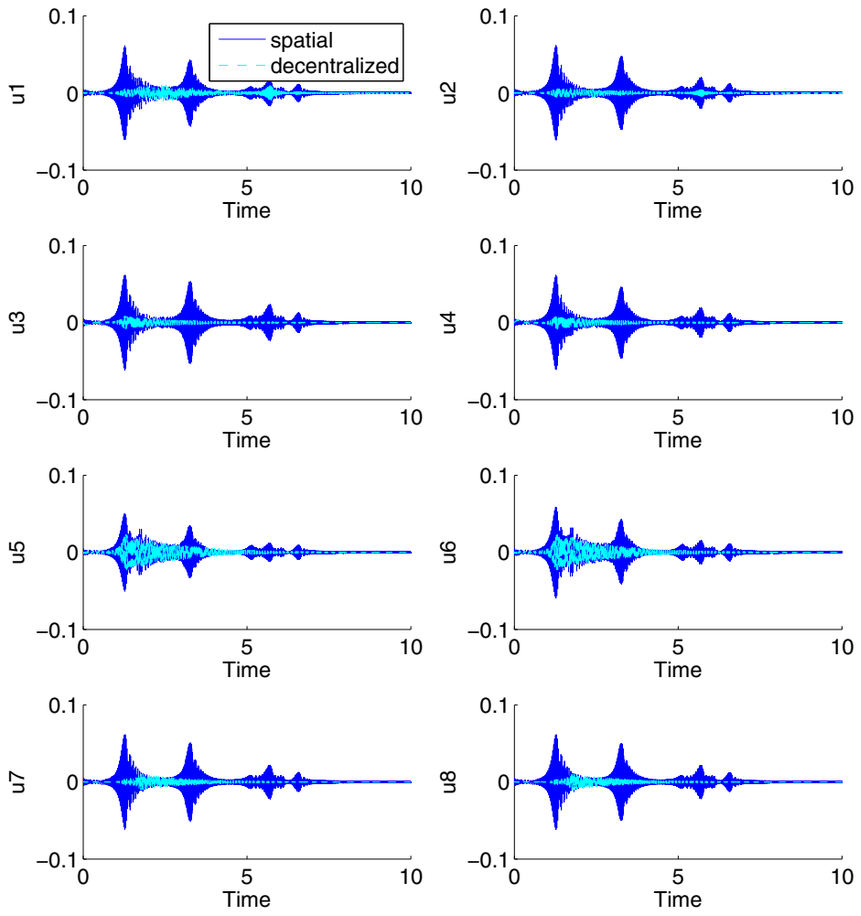

Fig. 10. Comparison of control signal in time domain between spatial and decentralized control

8. Concluding remarks

Two recently proposed $\mathcal{H}_\infty$ controller design methods dedicated to active structural vibration control were presented, and simulated results based on a finite element model of a plate were analyzed. The spatial norm based method aims to attenuate the vibration over entire regions of the structures, using the controller energy in a more effective way. The decentralized control method also tries to achieve a good energy distribution based on the application of the control effort through different controllers. A third controller, based on a standard $\mathcal{H}_\infty$ design for the complete plate, and using the same sensors and actuator, was evaluated also, to serve as a comparison base.

The decentralized control presented a similar behavior to the centralized one, but with a somewhat smaller control effort. Centralized control can demand more expensive equipment and is less robust in case of failures when compared to the decentralized approach. The results validate the option for a decentralized control as opposed to the regular centralized control.

The spatial control as compared to the decentralized control presented the better results in terms of attenuation. The analysis was based on the response on the same punctual performance points, instead of the complete region. But it is possible to affirm that a better attenuation on the complete region is present on the performance of this controller, based on the mathematical definition of the spatial norm.

A future investigation is related to the stability of the decentralized case, since each decentralized control can affect the others. In this work, this aspect was checked by the direct verification of the closed-loop stability, but only for the specific configuration of the four decentralized controllers considered here.

Also the choice of weighting function in the spatial control is an open problem, that heavily depends on the problem's practical requirements.

9. References

Balas, M. J. (1978). Feedback control of flexible systems, *IEEE Transactions on Automatic Control* 23: 673 - 679.

Barrault, G., Halim, D., Hansen, C. & Lenzi, A. (2007). Optimal truncated model for vibration control design within a specified bandwidth, *International Journal of Solids and Structures* 44(14-15): 4673 – 4689.

Barrault, G., Halim, D., Hansen, C. & Lenzi, A. (2008). High frequency spatial vibration control for complex structures, *Applied Acoustics* 69(11): 933 – 944.

Bathe, K.-J. (1995). *Finite Element Procedures (Part 1-2)*, Prentice Hall.

Baz, A. & Chen, T. (2000). Control of axi-symmetric vibrations of cylindrical shells using active constrained layer damping, *Thin-Walled Structures* 36(1): 1 – 20.

Bhattacharya, P., Suhail, H. & Sinha, P. K. (2002). Finite element analysis and distributed control of laminated composite shells using lqr/imsc approach, *Aerospace Science and Technology* 6(4): 273 – 281.

Bianchi, E., Gardonio, P. & Elliott, S. J. (2004). Smart panel with multiple decentralized units for the control of sound transmission. part iii: control system implementation, *Journal of Sound and Vibration* 274(1-2): 215 – 232.

Boyd, S., El Ghaoui, L., Feron, E. & Balakrishnan, V. (1994). *Linear Matrix Inequalities in System and Control Theory*, Vol. 15 of *Studies in Applied Mathematics*, SIAM.

Casadei, F., Ruzzene, M., Dozio, L. & Cunefare, K. A. (2010). Broadband vibration control through periodic arrays of resonant shunts: experimento investigation on plates, *Smart materials and structures* 19.

Cheung, Y. & Wong, W. (2009). H_∞ and H_2 optimizations of a dynamic vibration absorber for suppressing vibrations in plates, *Journal of Sound and Vibration* 320(1-2): 29 – 42.

Ewins, D. J. (2000). *Modal Testing: Theory, Practice and Application*, Research Studies Press, Ltd.

Ferreira, A. (2008). *MATLAB Codes for Finite Element Analysis: Solids and Structures*, Springer Publishing Company, Incorporated.

Gawronski, W. (2004). *Advanced Structural Dynamics and Active Control of Structures*, Springer-Verlag.

Halim, D. (2002). *Vibration analysis and control of smart structures*, PhD thesis, University of NewCastle – School of Electrical Engineering and Computer Science, New South Wales, Australia.

Halim, D. (2007). Structural vibration control with spatially varied disturbance input using a spatial method, *Mechanical Systems and Signal Processing* 21(6): 2496 – 2514.

Halim, D., Barrault, G. & Cazzolato, B. S. (2008). Active control experiments on a panel structure using a spatially weighted objective method with multiple sensors, *Journal of Sound and Vibration* 315(1-2): 1 – 21.

Hurlebaus, S., Stöbener, U. & Gaul, L. (2008). Vibration reduction of curved panels by active modal control, *Comput. Struct.* 86(3-5): 251–257.

Jiang, J. & Li, D. (2010). Decentralized guaranteed cost static output feedback vibration control for piezoelectric smart structures, *Smart Materials and Structures* 19(1): 015018.

Qu, Z.-Q. (2004). *Model Order Reduction Techniques with Applications in Finite Element Analysis*, Springer.

Skelton, R. E., Iwasaki, T. & Grigoriadis, K. M. (1998). *An Unified Algebraic Approach to Linear Control Design*, Taylor and Francis.

Zhou, K. & Doyle, J. C. (1997). *Essentials of Robust Control*, Prentice Hall.

Zilletti, M., Elliott, S. J. & Gardonio, P. (2010). Self-tuning control systems of decentralised velocity feedback, *Journal of Sound and Vibration* 329(14): 2738 – 2750.

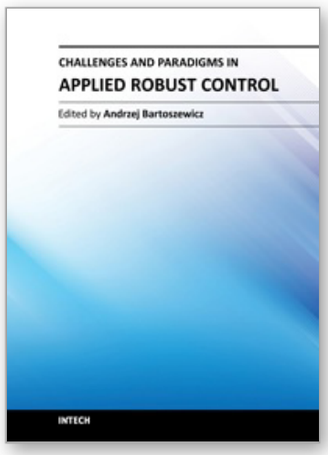

Challenges and Paradigms in Applied Robust Control

Edited by Prof. Andrzej Bartoszewicz

ISBN 978-953-307-338-5
Hard cover, 460 pages
Publisher InTech
Published online 16, November, 2011
Published in print edition November, 2011

The main objective of this book is to present important challenges and paradigms in the field of applied robust control design and implementation. Book contains a broad range of well worked out, recent application studies which include but are not limited to H-infinity, sliding mode, robust PID and fault tolerant based control systems. The contributions enrich the current state of the art, and encourage new applications of robust control techniques in various engineering and non-engineering systems.

How to reference

In order to correctly reference this scholarly work, feel free to copy and paste the following:

Alysson F. Mazoni, Alberto L. Serpa and Eurípedes G. de O. Nóbrega (2011). A Decentralized and Spatial Approach to the Robust Vibration Control of Structures, Challenges and Paradigms in Applied Robust Control, Prof. Andrzej Bartoszewicz (Ed.), ISBN: 978-953-307-338-5, InTech, Available from: http://www.intechopen.com/books/challenges-and-paradigms-in-applied-robust-control/a-decentralized-and-spatial-approach-to-the-robust-vibration-control-of-structures

INTECH
open science | open minds

InTech Europe
University Campus STeP Ri
Slavka Krautzeka 83/A
51000 Rijeka, Croatia
Phone: +385 (51) 770 447
Fax: +385 (51) 686 166
www.intechopen.com

InTech China
Unit 405, Office Block, Hotel Equatorial Shanghai
No.65, Yan An Road (West), Shanghai, 200040, China
中国上海市延安西路65号上海国际贵都大饭店办公楼405单元
Phone: +86-21-62489820
Fax: +86-21-62489821

IntechOpen